

## Influence of defects on cathodoluminescence along $\text{ZnTe}_x\text{O}_{1-x}$ -ZnO microstructures grown by the vapour-solid technique

A. Iribarren<sup>a, b†</sup>, P. Fernández<sup>b</sup>, and J. Piqueras<sup>b</sup>

a) Instituto de Ciencia y Tecnología de Materiales, Universidad de La Habana, Zapata y G, Vedado, Ciudad de La Habana 10440, Cuba; agosto@fisica.uh.cu

b) Departamento de Física de Materiales, Facultad de Ciencias Físicas, Universidad Complutense de Madrid, 28040, Madrid, España.

Received 15/07/2008. Approved in final version 07.05.2009.

**Sumario.** Se presenta el comportamiento de la emisión catodoluminiscente (CL) a lo largo de microestructuras alargadas de ZnO con impurificación isovalente de Te que fueron obtenidas por la técnica de vapor – sólido. La intensidad de la CL varía a lo largo de las microestructuras debido a la influencia de los defectos. Dos defectos principales fueron considerados, las vacancias y el desorden estructural. Cada defecto tiene diferente influencia sobre la intensidad de la CL, lo que se observa en el estudio de estructuras típicas seleccionadas. El grado de influencia de cada defecto fue analizado de los datos experimentales. Los tiempos de vida de recombinación en cada defecto fueron también estimados.

**Abstract.** The behaviour of the cathodoluminescence (CL) along elongated ZnO microstructures with isoelectronic Te doping, which were obtained by the vapour – solid technique is presented. The CL intensity changes along the microstructures due to the influence of the defects. Two main defect kinds were considered, the vacancy and the structural disorder. Each defect kind has different influence on the CL intensity, which is observed in the study of selected typical structures. The degree of influence of each defect was analysed from the experimental data. The recombination lifetimes for each defect were also estimated.

**Palabras clave.** Te-doped ZnO 61.72.uj, Cathodoluminescence 72.20.Jv, Defects 71.55.Gs

### 1 Introduction

The main and most observed defects of ZnO are those consequence of vacancies, mainly related to oxygen ones ( $\text{V}_\text{O}$ )<sup>1</sup> and its complexes. Such vacancies induce the formation of deep trap levels into the band gap. The transitions to these deep levels give a wide band centred at about 2.35–2.4 eV that ranges from 1.7 to 2.8 eV<sup>2</sup> in luminescence spectra. Under certain obtaining conditions of ZnO structures, as the isovalent doping that passivates the vacancies, the defect band is not present<sup>3</sup>; however structural disorder can be present and form band tails,

which favours non radiative mechanisms and lowering of the luminescence emission. In this work the study of the influence of both defect types, the vacancy and the disorder ones, was carried out from the behaviour of the cathodoluminescence (CL) emission spectra along Te doped ZnO microstructures grown by vapour-solid technique and, from them, and the carrier lifetime associated to each defect was estimated and compared.

### 2 Experimental

The raw materials were commercially available ZnO and

TeO<sub>2</sub> powders, which were mixed. The TeO<sub>2</sub> concentrations corresponded to 0.18 at.% Te. The mixed powders were milled for 10 h in a Retsch S100 centrifugal agate balls mill. Afterwards, the milled powders were compacted under a 2 T compressive load to form disc-shaped samples of about 7 mm diameter. The samples were then placed on an alumina boat near the gas inlet in a furnace, and sintered at 1270 °C under 2 litres per minute argon flow for 15 hours. Structure and morphology were investigated by scanning electron microscopy (SEM) in a Leica 440. CL measurements were carried out at room temperature on a Leica 440 SEM, and were carried out at constant exposure time and measured area. CL images were recorded by using a Hamamatsu R928 photomultiplier and CL spectra were obtained with a Hamamatsu PMA-11 CCD camera. X-ray microanalysis was performed using a JEOL JXA-8900 Superprobe by EDS.

For this study two main parameters were used and obtained from the spectra correspondingly. One of them is the integrated CL emission,  $A$  with a proper subscript, given by the area under the corresponding CL emission. The other one is the band tail parameter,  $E_0$ , given by the exponential fitting of the low energy side of the corresponding CL peaks<sup>4</sup>.

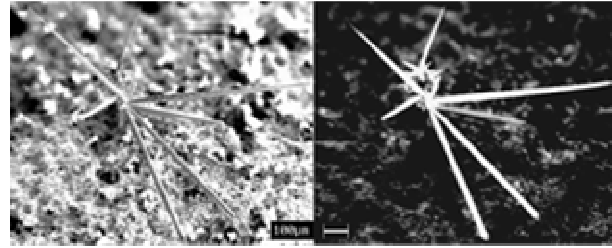
### 3 Results and discussion

**3.1 Influence of structural disorder.** In needle- and pencil-like microstructures, which are typical in the sample centre, shown in Figure 1 the defect band is not present, and they present a unique violet band due to ZnTe<sub>x</sub>O<sub>1-x</sub> and some ZnO as can be observed in the CL spectra in Figure 2. However, Figure 2 shows that CL emission intensity diminishes as the band tail  $E_0$  increases, which takes place from the microstructure base to the tip. It indicates that the structural disorder described by  $E_0$  increases in such a way. The disorder would be related to strain and formation of states near the top of the valence band due to isovalent and less electronegative Te atoms in O sites<sup>5</sup>.

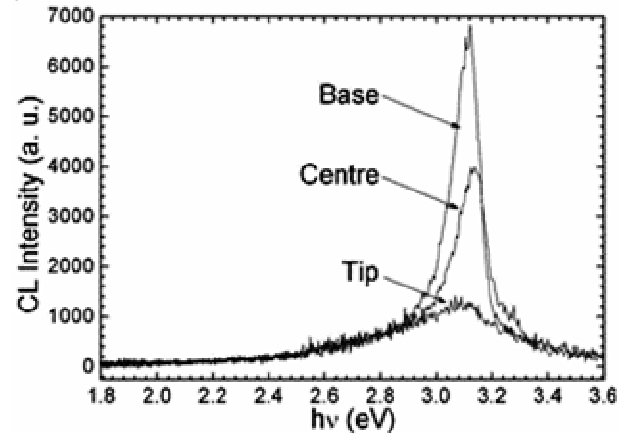
The main violet CL emission band is composed typically by two contributions, one at about 3.27 eV corresponding to transition in ZnO and the other one at 3.12 eV, which have higher intensity, corresponding to ZnTe<sub>x</sub>O<sub>1-x</sub><sup>1</sup>. The ZnO emission intensities were observed to be lower than that of ZnTe<sub>x</sub>O<sub>1-x</sub>. This is explained from the lower ZnO recombination coefficient, related to a typical recombination lifetime  $\tau_{\text{ZnO}} \sim 100$  ps, respect to that of ZnTe<sub>x</sub>O<sub>1-x</sub>,  $\tau_{\text{ZnTeO}} \sim 30$  ps<sup>5,6</sup>.

Figure 3 displays the behaviour of the integrated CL emission  $A_T$  as a function of the band tail parameter  $E_0$ , which was exponentially fitted. It shows that for high  $E_0$  the emission decreases up to minimal value  $A_T$  and conversely it would reach a maximum one. It indicates that the increase of the density of states in the band tail leads to the increase of the transitions through it, which would have lower transition probability. For high tail parameters the CL emission tends to a minimum value of the

emission  $A_{T\text{tail}}$  due to all the transitions take place mainly through the band tail.



**Figure 1.** SEM and CL images of ZnTe<sub>x</sub>O<sub>1-x</sub> - ZnO needle- and pencil-like microstructures located in the sample centre region.



**Figure 2.** CL spectra along a needle-like microstructure.

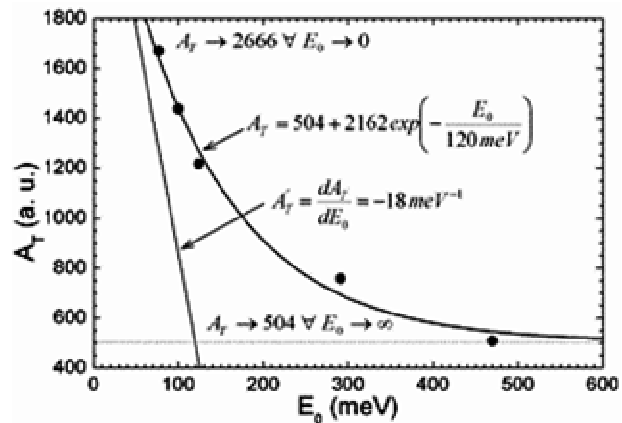


**Figure 3.** Behaviour of the total CL integrated emission area ( $A_T$ ) as a function of the ZnTe<sub>x</sub>O<sub>1-x</sub> band tail parameter ( $E_0$ ) in a needle-like microstructure.

For this case, recombination through deep levels can be neglected and a unique radiative transition from ZnTe<sub>x</sub>O<sub>1-x</sub> conduction to valence bands can be considered. For low band tail parameter,  $E_0 \rightarrow 0$ , i. e., in a nearly perfect material, the emission intensity  $A_{T0}$  is related to the recombination constant  $\gamma_{\text{ZnTeO}}$  and the excited carrier concentration that occupy states in the band,  $N_0$ . From experiment it can be represented by:

$$A_{T0} = 2666 \propto \frac{N_0}{\tau_{ZnTeO}}. \quad (1)$$

For very disordered material with high  $E_0$ , i. e.,  $E_0 \rightarrow \infty$ , the density of localized states in the tails is so high that it can be grossly considered that the same carrier concentration  $N_0$  occupies states only in the band tail. Then, the emission intensity can be given by:

$$A_{Ttail} = 504 \propto \frac{N_0}{\tau_{tail}}. \quad (2)$$

From comparing Eqs. 1 and 2, and using the  $\tau_{ZnTeO}$  value, it is possible to estimate that the carrier lifetime in the tail localized states is about  $\tau_{tail} \sim 160$  ps.

**3.2 Influence of the vacancies.** The mace-like microstructures displayed in Figure 4 have high CL emission in the tip region and it diminishes toward the base due to the increase of the defect concentrations related to the increase of the defect CL emission as can be observed in Figure 5. EDS measurements showed that the Te content decreases from tip to base<sup>3</sup>, i.e., less Te amounts lead low passivation of the O vacancies toward the base. The presence of vacancy defects leads to non radiative transition through the deep trap levels related to them.

The wide defect emission band centred at about 2.36 eV, is due to several transitions through deep trap levels<sup>1</sup>. The complexity of this band prevents a clear definition of the emission processes. The recombination constants related to defects have been reported ranging from high values corresponding to recombination lifetimes as short as  $\tau_{def} \sim 30$  ps, to high ones as long as minutes and hours<sup>6,8-10</sup>.

The  $ZnTe_xO_{1-x} - ZnO$  CL emission in the mace-like microstructures quickly decays as the defect band increases until a minimum emission, which takes place practically only in transitions through the defect levels. Further studies are necessary for attain a full description of the defect band emission processes. However, an effective recombination lifetime of vacancy defect can be grossly estimated. The tail parameters of the  $ZnTe_xO_{1-x}$  emission peak in mace-like microstructures range from 68 meV to 90 meV. This short range can be explained from the lattice relaxation in the vacancy complex centres. According to the previous calculus,  $E_0$  values would lead to 35 % – 43 % reduction of the emission intensity. However, the sharp experimental reduction of the emission as defect band increases suggests that the dominant mechanism for the reduction of the  $ZnTe_xO_{1-x} - ZnO$  CL emission is by transitions through vacancy defects. For the study it was defined a parameter  $r$  given by the ratio of the integrated defect emission  $A_{def}$  and the integrated  $ZnTe_xO_{1-x} - ZnO$  emission  $A_{ZnTeO-ZnO}$ . Thus, the integrated total emission  $A_{T0}$  was plotted as a function of such parameter  $r$  in Figure 6, and the experimental points were exponentially fitted. According to the fitting curve, if no defects are present ( $r \rightarrow 0$  or  $A_{def} \rightarrow 0$ ), the total emission  $A_{T0}$  is mainly related to the excited carrier con-

centration in the conduction band,  $N_0$ , and:

$$A_{T0} = 2105 \propto \frac{N_0}{\tau_{ZnTeO}}. \quad (3)$$

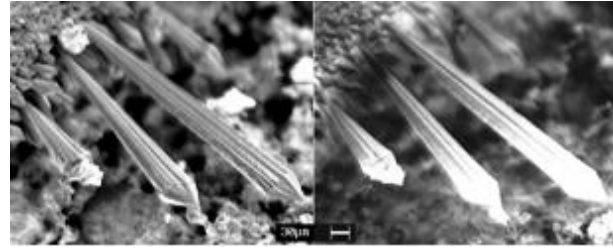


**Figure 4.** SEM and CL images of  $ZnTe_xO_{1-x} - ZnO$  mace-like microstructures located in the sample rim region.

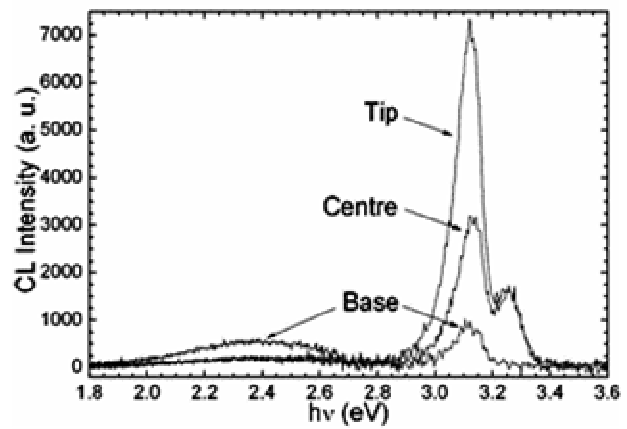


**Figure 5.** CL spectra along one of the mace-like microstructures.

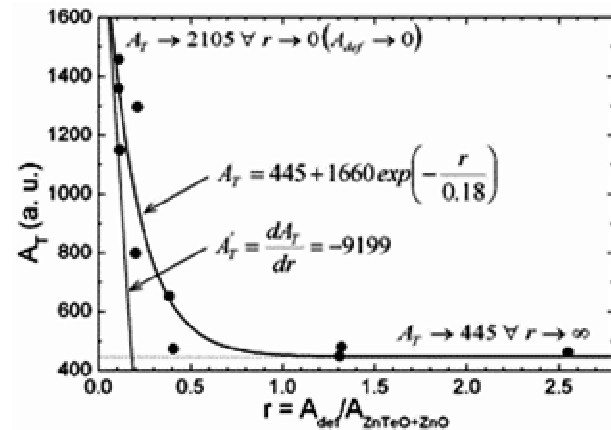


**Figure 6.** Behaviour of the total CL integrated emission area ( $A_T$ ) as a function of the ratio  $r$  between the  $ZnTe_xO_{1-x} - ZnO$  and the defect CL integrated emission areas.

At the high- $r$  asymptotic extreme, only defect transitions can be considered to take place. In this case a further consideration must be done, which is that the deep level concentration is so high that reach similar values to  $N_0$ , i.e.,  $N_{def} \sim N_0$ , and as the same excited carriers inter-

vene in the transitions to traps, the emission can be given as:

$$A_{\text{Tdef}} = 445 \propto \frac{N_0}{\tau_{\text{def}}} \quad (4)$$

From Eqs. 3 and 4 the effective recombination lifetime of the carriers in transitions through deep trap levels was estimated to be  $\tau_{\text{def}} \sim 145$  ps. This value can not be thought about even an average, because the transitions are multiples, including band-deep level, deep level-deep level, and other emission and absorption transitions, aside from the lifetime of each trap depends exponentially on its energy position within the band gap<sup>11,12</sup>.

**3.3 Comparison of defect influences.** The first order terms of the expansion to series of the total integrated emission area dependences on  $r$  and  $E_0$  respectively, which are displayed in the Figs. 3 and 6, give the rate of CL diminishing,  $A'_T = \frac{dA_T}{dr}$  for the vacancy defects in the region of low defect concentrations and

$A'_T = \frac{dA_T}{dE_0}$  for the disorder defects as a function of  $E_0$  in

the region of low disorder. In the needle- and pencil-like microstructures, where no defect CL bands are present, the CL emission diminishing represented by its  $A'_T$  is softer than that of maze-like structure where the main influence on the CL emission are the vacancy defects, which is sharper. This is related to the vacancy defects stronger influence of the vacancy defect on the total emission diminishing and the quick increase of the vacancy concentration from base to tip. The fact that the vacancy defects are luminescent and contribute to the total emission strengthen that assumption, meanwhile the disorder-defects increase reduces the transition probability without luminescence contribution.

On the other hand, the estimated effective recombination lifetime of the transitions through the band tails is some higher than that of the transitions through the vacancy defects. However, due to the proper nature of the recombination lifetime in the vacancies, some of them individually must have either higher values or lower ones.

The described behaviours of the CL emission along the microstructures is associated to the structures grow at high temperatures, which stimulate the evaporation of the initial source compound, ZnO and TeO<sub>2</sub>. However the growing structures in the internal zone of the ZnO substrate have an environment with high concentration of the source compounds, which decreases toward the rim. Thus the structures at the centre of the substrate, as the needle- and pencil-like ones, tend to be Te passivated and those near the rim have a concentration gradient, as in the maze-like microstructures. Additional concentration gradient can be expected if the microstructures grow and distance from the substrate surface, which was ob-

served in other microstructures not presented in this work.

## 3 Conclusions

The influence of the two main defect kinds, vacancies and structural disorder, on the CL emission was studied along ZnTe<sub>x</sub>O<sub>1-x</sub> - ZnO microstructures. The vacancy defects lead to the presence of deep levels through which the transitions take place, compete with the band to band transitions and diminish the CL emission. When the isovalent Te passivates the vacancies the defect CL emission decreases, but it was found that if the structural disorder increases the states of band tails also increase and the transitions through the band tails compete with that of the conductivity band and the CL emission also diminishes. However, the vacancy defects have higher influence on the CL emission diminishing than the structural disorder. From experimental data the tail and the defect recombination lifetimes were estimated.

## Acknowledgements

One of the authors (A.I.) would like to thank MEC and Universidad Complutense de Madrid, Spain, for a research grant under SAB2005-0018. This research was partially supported by Project MAT2006-01259 and it is also under Project PNCIT 00613457.

## References

1. A. Iribarren, P. Fernández, J. Piqueras, Superlattice and Microstructures 43, 600 (2008), and references therein.
2. J. Grym, P. Fernández and J. Piqueras, Nanotechnology 16, 931 (2005).
3. A. Iribarren, P. Fernández, J. Piqueras, J. Mater. Sci. 43, 2844 (2008).
4. A. Iribarren, R. Castro-Rodríguez, V. Sosa., J.L. Peña, Phys. Rev. B 60, 4758 (1999).
5. H.J. Liu, C.T. Chan, Phys. Lett. A 352, 531 (2006).
6. H. L. Porter and J. F. Muth, J. Narayan, John V. Foreman and Henry O. Everitt, J. Appl. Phys. 100, 123102 (2006).
7. G. A. Garrett, H. Shen, M. Wraback, L. Tsakalacos, S. F. LeBoeuf. CLEO '07. 2007 Conference on Lasers and Electro-Optics. IEEE, pp. 907-8. Piscataway, NJ, USA.
8. T.E. Murphy, K. Moazzami and J.D. Phillips, J. Electron Mater. 35, 543 (2006).
9. Zh. Fan, P.-ch. Chang, J. G. Lu, E. C. Walter, R. M. Penner, Ch.-h. Lin, H. P. Lee, Appl. Phys. Lett. 85, 6128 (2004).
10. Ü. Özgür, A. Teke, C. Liu, S.-J. Cho, and H. Morkoç, H. O. Everitt, Appl. Phys. Lett. 84, 3223 (2004).
11. A. Muller, P. Bianucci, C. Piermarocchi, M. Fornari, I. C. Robin, R. André, and C. K. Shih, Phys. Rev. B 73, 081306(R) (2006).
12. A. Gupta, H. S. Bhatti, D. Kumar, N. K. Vermaa, R. P. Tandon, Digest J. Nanomater. Biostruct. 1, 1 (2006).